

Ale Formulation with Explosive Mass Scaling for Blast Loading: Experimental and Numerical Investigation

Souli M.¹, Bouamoul A.² and Nguyen-Dang T.V.³

Abstract: Protection of military vehicles against blast mine and high explosive in air is of a great concern in defence industry. Anti-Vehicle (AV) mines and Improvised Explosive Devices (IED's) are capable of inflicting damage to heavy vehicles. For the last decades, numerical simulation of blast wave propagation and its interaction with surrounding structures becomes more and more the focus of computational engineering, since experimental tests are very expensive and time consuming. This paper presents an experimental and numerical investigation of blast wave propagation in air, using an Arbitrary Lagrangian Eulerian (ALE) multi-material formulation developed in LS-DYNA with the contribution of the first author. To accurately capture peak pressure values of the shock wave, a very fine mesh, in the explosive material and the surrounding air mesh, is needed. For three dimensional problems, this condition leads to large size problems that can be CPU time consuming and not appropriate to run several times for engineering design purposes and structure analysis to resist blast loading. In order to calibrate numerical models to experimental data, using reasonable fine mesh, explosive masse scaling is used in this paper. Good correlations in terms of pressure and impulse between numerical results and experimental data were obtained when using the right combination of solution parameters and multiplying the explosive mass by an appropriate scaling factor. This procedure is commonly used in defence industry for structural design and to avoid running large scale problems.

1 Introduction

Simulation of blast wave propagation and its interaction with the surrounding structures becomes more and more the focus of computational engineering in defence industry. It is well known that experimental tests of high explosive detonation and impact on surrounding structures are expensive and time consuming. To reduce the

¹ Université de Lille1, Laboratoire de Mécanique de Lille, UMR CNRS 8107

² Defence Research and Development Canada - Valcartier Québec, Qc G3J 1X5.

³ Université Laval, Québec, Qc, Canada

number of experimental tests, theoretical and experimental studies of blast wave have been considered by several researchers over the past decades. When a high explosive is detonated an inward wave is generated in the explosive material, at the same time, a shock wave moves through the air medium, which is at lower pressure and a contact discontinuity appears between the rarefaction wave and the shock wave. Experiments have shown that the resulting flow is quite complex, involving several physical phenomena as burning effects and heat transfer. The detonation of high explosive material converts the explosive charge into gas at high pressure and temperature what leads to high structures damage. Numerical simulations help to minimize the number of tests required which are very costly, and also help to interpret test results. Once simulations are validated by test results, it can be used as design tool for the improvement of the system structure involved. In defence industry, classical Lagrangian finite element methods have been used to solve blast problems and pressure propagation, but the Lagrangian formulation cannot resolve large deformations very accurately. Recent development such as ALE or Eulerian multi-material formulations can be used as an alternative for the simulation of high explosive phenomena. ALE formulations have been developed to overcome the difficulties due to large mesh distortion. The ALE multi-material formulation developed in LS-DYNA code, see Hallquist (1998), by the first author and used in this paper, has been validated for several academic and industrial applications. The formulation has been implemented in the LS-DYNA explicit finite element code to be able to simulate fluid structure interaction problems, where the fluid mesh can be defined by an ALE or Eulerian mesh and the structure mesh as a Lagrangian deformable mesh. In the ALE multi-material formulation, a fluid element can contain more than one material. For explosive detonation in ambient air, an element may contain two different materials, explosive and air, with their respective volume fractions in the element. During the simulation, state variables are computed and stored for each material in each element. An interface tracking an algorithm based on Young's method (1982) is used to capture the interface between the two materials inside the element. This method was used successfully to model many industrial and academic applications as sloshing tank problem as described in Aquelet *et al* (2006).

For the simulation of blast wave interacting with a surrounding structure, pressure values need to be computed accurately for structure loading. To accurately capture peak pressure values of the shock wave, a very fine mesh with element size of the order of 1 mm, in the explosive material and the surrounding air mesh, is needed. For three dimensional problems, this condition leads to large size problem that can be CPU time consuming and not appropriate to run several times for engineering design and structure analysis to resist blast loading. In order to calibrate the nu-

merical models to experimental data, using reasonable fine mesh, explosive mass scaling is used. Once simulations are validated by test results, it can be used as a design tool for the improvement of the system structure involved.

In this paper, we describe in Section 2, the ALE formulation of the Navier-Stokes equations in an arbitrary moving domain, and the advection algorithms used to solve mass, momentum and energy conservation. In Section 3, description of High explosive and related JWL (Jones-Wilkins_Lee) equation of state are highlighted. These equations are commonly used to evaluate pressure shock wave at pressure sensors located far away from the detonation point. To assess mesh sensitivity of the described problem, different mesh sizes have been used for peak pressure enhancement. In order to capture peak pressure accurately, and minimize energy dissipation and diffusion, very fine mesh needs to be used in the simulation. This may lead to large size problems mainly for three dimensional problems that may take several days to run even with multiple processors. For design purposes where several runs are required, this procedure cannot be used. In order to use moderate size problems, and compensate for energy dissipation, high explosive mass scaling is introduced and described in Section 4.

2 ALE and Eulerian Multi-material formulations

Fluid problems, in which interfaces between different materials (e.g. gas and ambient air) are present, are more easily modeled using a Lagrangian mesh. However, if an analysis for complex geometry is required, the distortion of the Lagrangian mesh makes such a method difficult to use and many re-meshing steps are necessary for the calculation to continue. Another method to use is the Eulerian formulation. This change from a Lagrangian to an Eulerian formulation, however, it introduces two problems. The first one is the interface tracking Young (1982), and the second is the advection phase or advection of fluid material across element boundaries.

To solve these problems, an explicit finite element method for the Lagrangian phase and a finite volume method (i.e. flux method) for the advection phase are used. For a full description of the explicit finite element method, the authors refer to the following explicit codes: Pronto, Dyna3D and LS-DYNA;. The advection phase has been developed by the first author into the LS-DYNA code, extending the range of applications that can be used with the ALE formulation. Current applications include sloshing involving a 'free surface', and high velocity impact problems where the target is modeled as a fluid material, thus providing a more realistic representation of the impact event by capturing large deformations.

An ALE formulation contains both pure Lagrangian and pure Eulerian formulations. The pure Lagrangian description is the approach that the mesh moves with

the material, making it easy to track interfaces and to apply boundary conditions. Using an Eulerian description, the mesh remains fixed while the material passes through it. Interfaces and boundary conditions are difficult to track using the last approach; however, mesh distortion is not a problem because the mesh never changes.

In the ALE description, an arbitrary referential coordinate is introduced in addition to the Lagrangian and Eulerian coordinates. The material derivative with respect to the reference coordinate can be described in Equation (2.1). Thus substituting the relationship between the material time derivative and the reference configuration time derivative derives the ALE equations.

$$\frac{\partial f(X_i, t)}{\partial t} = \frac{\partial f(x_i, t)}{\partial t} + w_i \frac{\partial f(x_i, t)}{\partial x_i} \quad (1)$$

In the last equation, X_i is the Lagrangian coordinate, x_i the Eulerian coordinate, w_i is the relative velocity. Let denote by v the velocity of the material and by u the velocity of the mesh. In order to simplify the equations, we introduce the relative velocity $w = v - u$. Thus, the governing equations for the ALE formulation are given by the following conservation equations (2.2) to (2.4):

(i) *Mass equation.*

$$\frac{\partial \rho}{\partial t} = -\rho \frac{\partial v_i}{\partial x_i} - w_i \frac{\partial \rho}{\partial x_i} \quad (2)$$

(ii) *Momentum equation.*

The strong form of the problem governing Newtonian fluid flow in a fixed domain consists of the governing equations and suitable initial and boundary conditions. The equations governing the fluid problem are the ALE description of the Navier-Stokes equations:

$$\rho \frac{\partial v_i}{\partial t} = \sigma_{i,j,j} + \rho b_i - \rho w_i \frac{\partial v_i}{\partial x_j} \quad (3)$$

Where σ_{ij} is the Cauchy stress tensor. Boundary and initial conditions need to be imposed for the problem to be well posed.

(iii) *Energy equation.*

$$\rho \frac{\partial E}{\partial t} = \sigma_{ij} v_{i,j} + \rho b_i v_i - \rho w_j \frac{\partial E}{\partial x_j} \quad (4)$$

Note that the Eulerian equations commonly used in fluid mechanics by the computational fluid dynamics (CFD) community, are derived by assuming that the velocity of the reference configuration is zero and that the relative velocity between

the material and the reference configuration is therefore the material velocity. The term in the relative velocity in equations (2.3) and (2.4) is usually referred to as the advective term, and accounts for the transport of the material past the mesh. It is the additional term in the equations that makes solving the ALE equations much more difficult numerically than the Lagrangian equations, where the relative velocity is zero.

In the second phase, the advection phase, transport of mass, internal energy and momentum across cell boundaries are computed. This may be thought of as remapping the displaced mesh at the Lagrangian phase back to its original or arbitrary position. From a discretization point of view of (2.2), (2.3) and (2.4), one point integration is used for efficiency and to eliminate locking. The zero energy modes are controlled with an hourglass viscosity described in Benson (1992). A shock viscosity, with linear and quadratic terms, is used to resolve the shock wave; a pressure term is added to the pressure in the energy and momentum equations (2.3) and (2.4). The resolution is advanced in time with central difference method, which provides a second order accuracy in time integration. For each node, the velocity and displacement are updated as follows:

$$u^{n+1/2} = u^{n-1/2} + \Delta t . M^{-1} . (F_{ext} + F_{int})$$

The multi-material formulation is attractive for solving a broad range of non-linear problems in fluid and solid mechanics, because it allows arbitrary large deformations and enables free surfaces to evolve. The Lagrangian phase of the volume of fluid VOF method is easily implemented in an explicit ALE finite element method. Before advection, special treatment for the partially voided element is needed. For an element that is partially filled, the volume fraction satisfies $V_f \leq 1$, and the total stress σ is weighed by volume fraction $\sigma_f = \sigma . V_f$. For a complete description of this method, the authors refer to xyz.

In the second phase, the transport of mass, momentum and internal energy across the element boundaries is computed. This phase may be considered as a ‘re-mapping’ phase. The displaced mesh from the Lagrangian phase is remapped into the initial mesh for an Eulerian formulation, or an arbitrary undistorted mesh for an ALE formulation. In this advection phase, the first author has solved a hyperbolic problem, or a transport problem, where the variables are density, momentum and internal energy per unit volume. Details of the numerical method used to solve the equations are described in detail in Aquelet et al (2005), where the Donor Cell algorithm, a first order advection method and the Van Leer algorithm, a second order advection method are used. As an example, the equation for mass conservation

would be :

$$\frac{\partial \rho}{\partial t} + \nabla \cdot (\rho u) = 0 \quad (5)$$

It is not the goal of this paper to describe the different algorithms used to solve equation (2.5); which are well described in in Aquelet et al (2005) but to used them to solve problems related to mass scaling for blast applications.

3 High Explosive Simulation

3.1 Material model and Equation of state for high explosive

In High explosive process, a rapid chemical reaction is involved, which converts the material into high pressure gas. From a constitutive material point of view, the gas is assumed to be inviscid with no shear, and the pressure is computed through JWL equation of state, a specific equation of state, commonly used for explosive materials. There have been many equations of state proposed for gaseous products of detonation, from simple theoretically to empirically based equations of state with many adjustable parameters Kingery et al (1984). The JWL equation of state determines the relation between blast pressure, change of volume and internal energy. The JWL equation of state was used in the following form:

$$P = A \left(1 - \frac{\omega}{R_1 V} \right) \exp(-R_1 V) + B \left(1 - \frac{\omega}{R_2 \omega} \right) \exp(-R_2 V) + \frac{\omega}{V} E \quad (6)$$

In Equation (3.1), P defines the pressure whereas V is the relative volume:

$$V = \frac{v}{v_0} \omega \quad (7)$$

In the late equation, v and v_0 are the current and initial element volume respectively, a , B , R_1 , R_2 and ω are material constants defined in Table 1. These performance properties are based on the cylinder expansion test done in controlled conditions. At the beginning of the computations, $V=1.0$ and E is the initial energy per unit volume.

The first term of JWL equation (a), known as high pressure term, dominates first for V close to one. The second term (B) is influential in the JWL pressure for V close to two. Note that in the expanded state, the relative volume is sufficiently important so that the exponential terms vanish, and JWL equation of state takes the form of an ideal gas equation of state (3.3):

$$P = \omega \frac{E}{V} \quad (8)$$

Table 1: High explosive parameters for C4

Parameter	Value
A, (MPa)	609.8
B, (MPa)	13.0
R1	4.5
R2	1.4
E, (MPa)	9.0
ω	0.25
Detonation velocity (m/s)	8193
Density, (kg/m ³)	1600
Chapman Jouget pressure, (MPa)	28

3.2 Material model and Equation of state for air

Air is modeled using the hydrodynamic material model. The model requires an equation of state, density, pressure cut-off and dynamic viscosity to be defined. The viscosity and pressure cut-off are set to zero, because pressure cannot be negative and the viscosity forces are negligible. The ideal gas law (i.e. gamma law) is used as an equation of state for air. This polytropic equation of state is given by considering the general linear polynomial equation of state (3.3):

$$P = (\gamma - 1) \frac{\rho}{\rho_0} E \quad (9)$$

Where ρ and $\rho_0 = 1 \text{ kg/m}^3$ are current and initial densities of air respectively, and E is the specific internal energy per unit volume (units of pressure) and γ is the polytropic ratio of specific heats. For the diatomic molecules comprising air, this adiabatic expansion coefficient is $\gamma = 1.4$. To be thermodynamically consistent, air must be initialized to atmospheric pressure. Note that from equation (3.3) at time $t=0$, for an initial pressure $P_0 = 0.1 \text{ MPa}$, the initial internal energy should be set to $E_0 = 1.25 \text{ MPa}$, since $\gamma = 1.4$, and $\rho = \rho_0$ at initial time. Setting a non-zero initial pressure in the air domain, appropriate boundary conditions are imposed at the external boundary, to avoid initial air leakage, thus a 0.1 MPa pressure boundary condition need to be assumed.

3.3 Blast wave propagation in ambient air

Blast waves are associated with rapid energy release processes such as explosions. Detonation of a high explosive (HE) is achieved by compressing and heating of the constituents. As a result, a chemical reaction is triggered and propagated supersonically at the Chapman-Jouget velocity through the explosive. The violent expansion

of the gaseous products generates a strong shock wave that propagates into the ambient medium. Shock waves are created because the sound speed increases with increasing temperature in a compressible flow. As a matter of fact, the wave travels faster than the sound speed in the ambient medium. The various properties of the fluid (e.g. density, pressure, velocity and Mach number) fluctuate almost discontinuously. In atmospheric conditions, with idealized specific heat ratio $\gamma=1.4$, the density and pressure across the shock increase whilst the speed decreases and the shock weakens as its Mach number decreases. When the flow Mach number becomes sonic $M = 1$, the jump in pressure, density and speed vanish and the shock fades away.

The typical pressure versus time curve at a stationary point (in the inertial reference frame) is presented in Fig. 1. The positive compression phase is characterized by a peak overpressure, P_s above that of the ambient medium, P_0 . The pressure immediately decays, as a function of time from its peak value. A negative expansion phase follows where the pressure drops below the ambient level. The time at which this shock occurs is termed the time of arrival, t_a . The duration of the shock, t_d , is the time between the time of arrival and the time at which the pressure reaches that ambient pressure. Another non-negligible aspect of a shock is its specific impulse, I , the momentum imparted in a blast. It can also be viewed as the area under the pressure-time curve.

$$I = \int_t P(t) dt \quad (10)$$

Its magnitude often determines structural damage and injuries caused by the blast. The duration of the shock increases with the distance from explosion, whereas the peak pressure decreases. With high-energy blasts, subsequent minor pressure maxima following the main one can be recorded although they are often disregarded because they occur with decreasing amplitude and are rapidly damped in the air. As the primary blast wave is moving outward, the expansion wave travels inward. When reflected at the blast center, the then created outward moving shock wave is referred to as the secondary shock. Tertiary shock can sometimes be observed since the cycle of compression and rarefaction is recurring periodically. Finally, reflections on grounds, walls or obstacles are much more likely to cause secondary and tertiary shocks than reflection of shock on itself. The internal structure of a shock front can be approximated by means of an equation of state together with the Rankine-Hugoniot relations that are based on the conservation of mass, momentum and energy through an adiabatic shock. These relations enable thermodynamic variables to be determined downstream as well as upstream.

3.4 Artificial bulk viscosity

Although they are mathematically treated as discontinuities, shocks do have a narrow thickness on the order of a few collision mean free path in the ambient gas. For air at STP (Standard Temperature and Pressure), the mean free path is estimated to 70 nanometer. Thus, to keep the accuracy of the results, the mesh size should be scaled until the shock is resolvable by each individual element. In practice, this method is not viable because the algorithm is requested to handle a massive amount of CPU time.

Furthermore, the equations of conservation of mass, momentum and energy across a shock require that kinetic energy be transformed into internal energy or heat. In the absence of physical viscosity in the immediate vicinity of the shock, an artificial unphysical one was added to dissipate the excess of energy. This has the effect of thickening the shock and smearing the discontinuity into a smooth transition zone, and thus, the shock is automatically captured on the computational mesh. As implied by its designation, the artificial viscosity possesses the basic properties of a real viscosity. This is a requirement to avoid significant unphysical results as described in Caramana, et *al* (1998). That is:

- it generates entropy and decreases kinetic energy (dissipative);
- it varies uniformly with the velocity field;
- it vanishes with uniform compression and rotation; and, it vanishes with sufficient expansion.

In LS-DYNA code, for each element, the artificial viscosity is formulated as follows:

$$Q = \rho h(C_0.h.(div(\vec{v}))^2) - C_1.a.hdiv(\vec{v}) \quad (11)$$

Where Q is a pressure term, added to the momentum and energy equations, C_0 and C_1 are dimensionless constants, h the mesh size of the element, and a the speed of sound in the element. The pressure term Q is only added for compression, when the divergence of the velocity is negative, $div(\vec{v}) < 0.$, and ignored for tension, $div(\vec{v}) > 0.$

4 Numerical Simulations

ALE formulation was used to treat high explosive blast propagation. All calculations were performed on Linux Workstation platform with Linux 2.4.21 operating

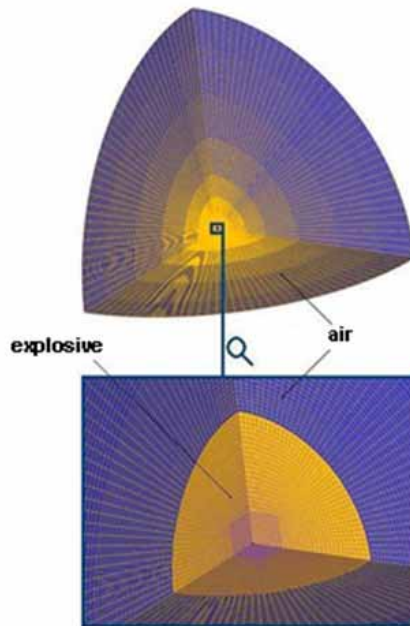


Figure 1: Finite element model with coarse mesh

system. The ALE blast model was explored by two means: comparison with experimental data published in open literature and comparison with numerical solutions based on a pure air blast calculation of above ground air-blast (no ground or reflections on obstacles were considered) of high explosives using CONWEP code, see Kingery, et *al* (1984). Various parametric studies were also conducted in order to correlate numerical results more closely to the experimental data and to assess model independence upon mesh characteristics.

4.1 Simulations using Spherical and cubic domains

Air-blast geometric model consists of two concentric spheres, the inner one being the explosive and the outer one representing the air (figure 1). A spherical explosive burst generates spherical blast waves expanding radially outward from the point source. Thus, for the modelling of the ambient medium, this geometry was preferred so as to ease radial wave propagation through the mesh. Given the prob-

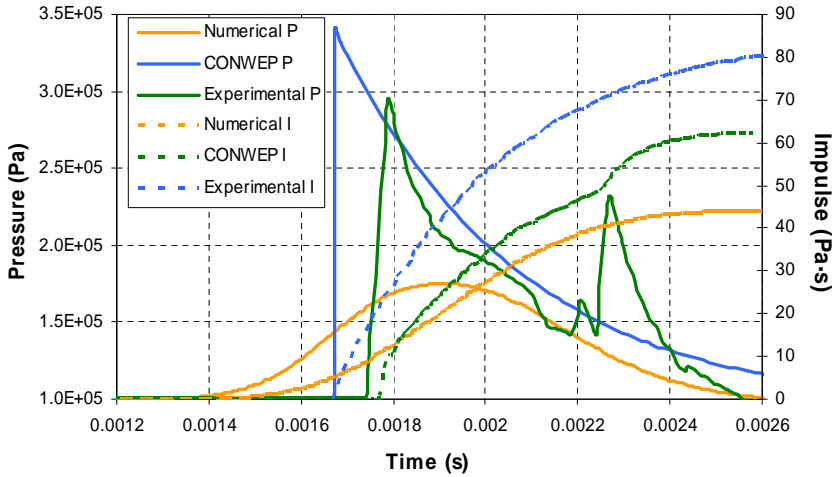


Figure 2: Comparison of numerical results (coarse mesh) with CONWEP and experimental data from Ref.3 (1lb C4). In the legend, P means pressure and I the impulse

lem symmetry, simplification of the model was possible by considering a sphere octant. As a result, symmetry conditions with 3 degree of freedom were set on nodes lying on every cutting plane. Moreover, initial pressure loading and non-reflecting boundary conditions corresponding were applied to all elements on the air-sphere free surface. Hence, pressure waves were dissipated from the mesh at the boundaries, therefore modelling an infinite domain. Air and explosive were discretized into hexahedron elements. Care had been taken to keep element lengths within reasonable range with the aim of maximizing computational precision without degrading the time step. The sphere octant was approximately 3 m radius and totalizing 302 000 elements, 270 000 for the air and 32 000 for the explosive. The element volume varied between $1.2 \text{ E}^{-10} \text{ m}^3$ and $6 \text{ E}^{-4} \text{ m}^3$. The explosive modelled for the purpose of this exploration was C4. Its radius was 0.0407 m with mass 0.454 kg (1 lb). C4 was modelled with the Jones-Wilkins-Lee (JWL) equation of state (Eq.3.14).

Pressure history from the numerical model was recorded at 200 kHz and 1.52 m from the center of explosion likewise the experimental one. Note that no artificial viscosity was used for these calculations. Comparison of the results with CONWEP and experimental data showed mediocre correlation (see Fig. 2). The pressure jump did not occur and the pressure value rose smoothly over a relatively long time lapse (~ 0.5 ms). The CONWEP peak pressure is 3.4 E^5 Pa, the experimental peak pressure is 2.8 E^5 Pa and the obtained numerical peak pressure is 1.8 E^5 Pa (repre-

senting -36% relative error). The numerical impulse is 44% less than the CONWEP impulse. In order to lighten the article, only comparisons with experimental result were made. The second peak of pressure observed in the experimental data was due to the reflection from the support of the charge (not ground) and was not modeled numerically.

4.2 Mesh sensitivity analysis

A series of meshes with various coarsenesses were created in order to conduct mesh sensitivity analysis. Details concerning these meshes are summarized in Fig. 3. Element ratio (i.e. its length divided by its width) was kept below 3:1 to ensure a three-dimensional analysis. As expected, better agreement between numerical and experimental results was achieved with increased mesh resolution. However, accuracy did not significantly increase from a 77 850- elements mesh to a 302 000-elements mesh (corresponding to a factor of 4), whereas the calculation cost increased appreciably. The elapsed time increased from 15 minutes to 1 hour 26 minutes and the memory usage quadrupled, all for a gain in accuracy on the peak pressure of only 9% (Fig. 5). Two experimental impulse curves were given in Fig. 4 (with and without support for the explosive). Since the support was not modeled, the numerical impulse was compared with the impulse curve corresponding to the one without the explosive support. For the three meshes, the impulse curves were different but with the same finale total impulse which was equal to 44.2 Pa.s representing -16% relative error regarding the experimental impulse (equal to 52.6 Pa.s). Only impulse curve of the coarse mesh is given in Fig. 4. Computational time and total memory usage for an explicit solution, when solving with single precision and using one processor are presented in Table 2. In addition, double precision calculations increased computational costs drastically without significantly affecting the results.

Artificial viscosity was added to the model using equation (3.4). For improved

Table 2: Computational cost and relative errors for various mesh-coarseness

	Coarse mesh	Fine mesh	Very fine mesh
Elements	56 700	77 850	302 000
Elapsed time Relative	13 min 21 s	14 min 56 s	1 h 26 min 02 s
Relative Error on peak overpressure	-36%	-31%	-27%
Relative Error on total impulse	-16%	-16%	-16%

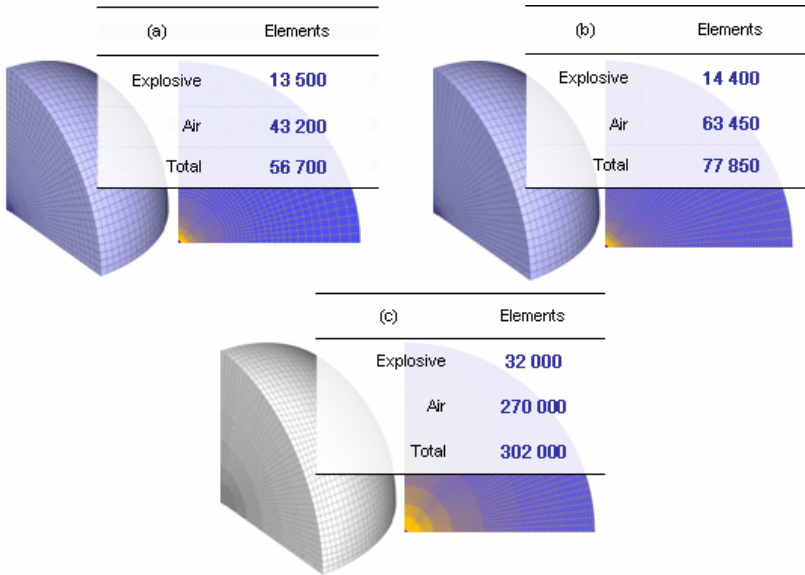


Figure 3: Total elements in coarse mesh (a), fine mesh (b) and very fine mesh (c)

results, a parametric study was performed to determine the quadratic coefficient C_o and its linear counterpart C_1 in equation (3.5). LS-DYNA default values are respectively 1.5 and 0.06. Various combinations of the coefficients were evaluated ($0.01 \leq C_o \leq 0.35$ and $0.001 \leq C_1 \leq 2.5$). As shown in Fig6, the peak pressure and the duration of the shock are both affected by artificial viscosity, whereas the total impulse is not. Better agreement with the experimental data was achieved when those coefficients were kept small, as high values resulted in excessive spreading of the shock. Oscillations behind the shock front intensify was observed when $C_o \leq C_1$. The maximum peak pressure, $2.17 E^5$ Pa, was obtained with $C_o = 0.09$ and $C_1 = 0.001$, therefore, the use of artificial viscosity results in a 4.5% improvement in the accuracy of the calculated peak pressure with a good approximation on the duration and pressure profile.

Because of the discrepancy between the experimental and the numerical pressure, a compensating scaling factor had to be prescribed to the explosive mass, the determination of its value being discussed in the next sub-section.

A cube-shaped domain with identical boundary conditions as the spherical and the same amount of explosive (1 lb of C4) was also used to assess numerical independence upon mesh geometry. Air and explosive were discretized into hexahedron

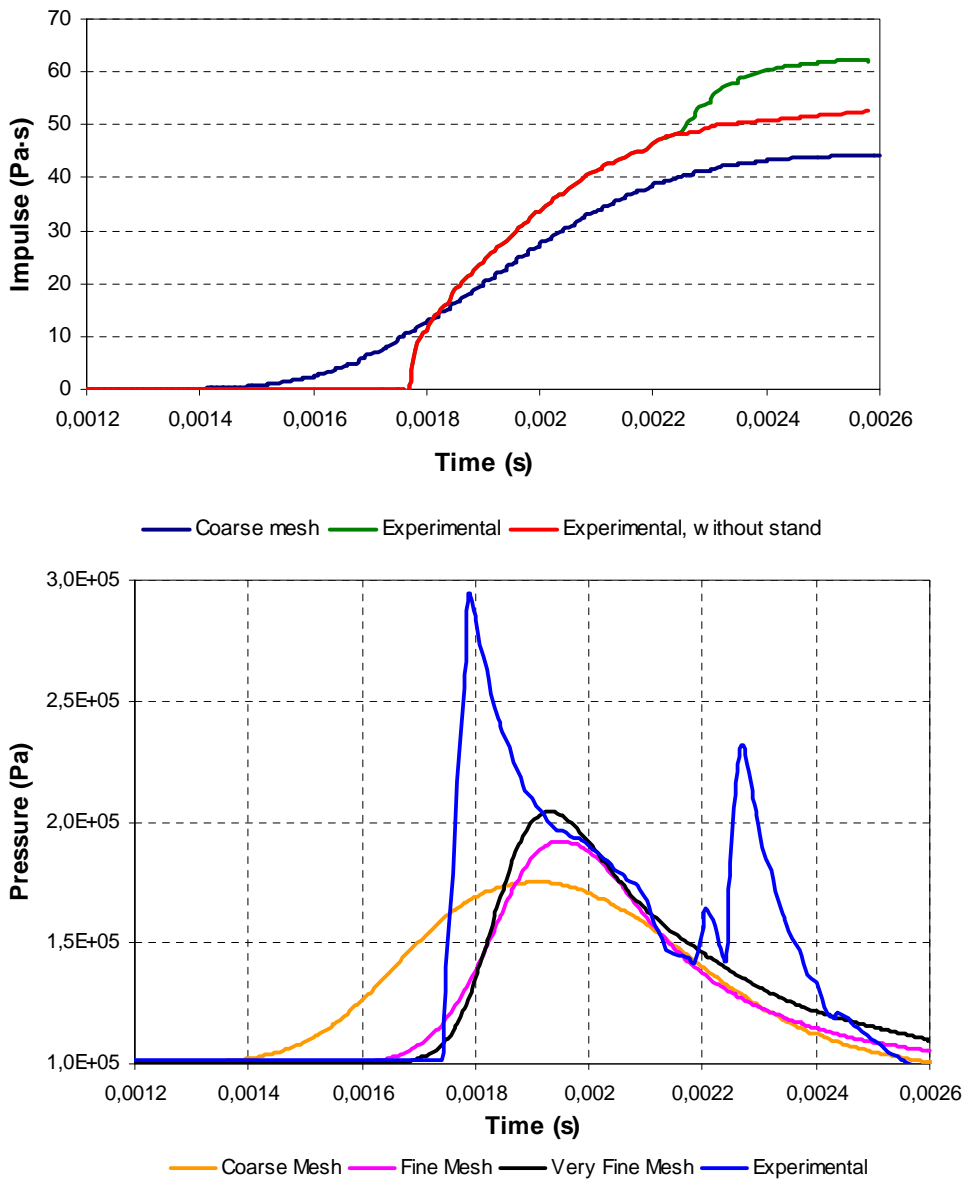


Figure 4: Pressure and impulse profiles for different mesh and from experiments (1 lb of C4 with stand)

elements. To achieve an effective comparison, element size in the cubic domain was matched with the dimensions of the elements at 1.52 m radial distance from the center coordinate in the spherical model. Figure 5 shows the cubical mesh model. Results were found to be identical, thus confirming numerical independence between these two types of meshing. For the following simulations, cube-shaped domain was used over the spherical-shape domain for flexibility of a cube to be meshed easily.

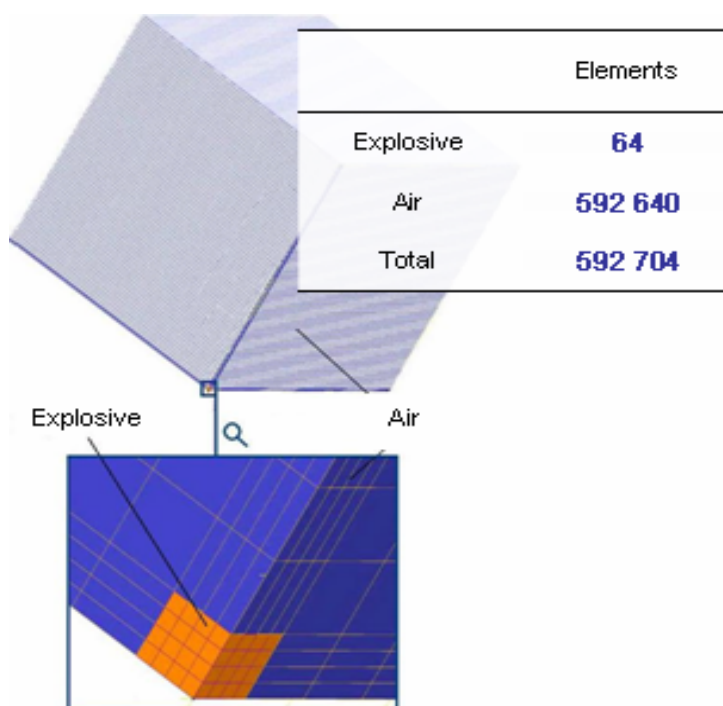


Figure 5: Cubical mesh

4.3 Explosive mass scaling

Using a cubic model developed previously, a parametric study was again conducted. The correlation between experimental data and the numerical model for the peak pressure and the impulse variable was assessed for various values of the explosive weight. Some inaccuracies were introduced into the results due to the mesh coarseness and to the inherent inaccuracy of the explosion is calculated on nodes although pressure is accounted in the centre of elements. Thus, uncertain-

ties were caused by an over or underestimation ($\pm 0.0167\text{m}$) of the distance from explosion.

The relative error between the maximum experimental overpressure and the numerical model was computed for scenarios in which the explosive mass (1 lb of C4) was multiplied by a scaling factor. Good results were obtained when this factor was equal to 1.18 as shown in Fig. 6. Finally, the simulation of small explosives (containing only a few elements) is to avoid as the inherent coarseness of the mesh may perturb the simulation of the pressure build-up in the explosive at detonation, thereby introducing a substantial error in the measured pressure of the surrounding air. Similarly, large radius explosives have to be modeled with care, for inexactness of the simulation data might arise due to near field effects

Since the ultimate objective is the design of structure resisting to load blast, numerical simulations can be included in shape design optimization with shape optimal design techniques Souli et al (1993), and material optimization Erchiqui et al (2007). Once simulations are validated by test results, it can be used as design tool for the improvement of the system structure being involved.

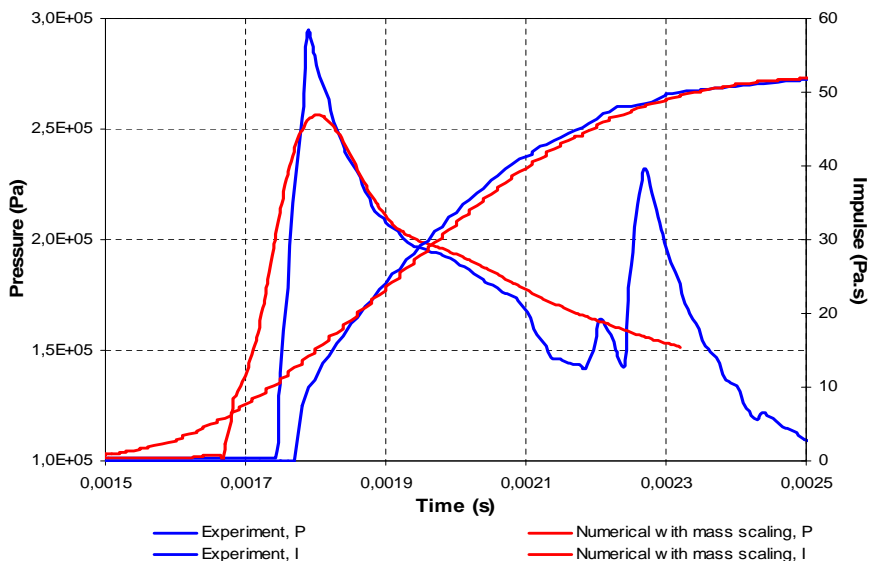


Figure 6: Comparison between experimental and the numerical pressure and impulse profile using a mass-scaling factor

5 Conclusion

In this work, we have presented the application of an Arbitrary Lagrangian Eulerian (ALE) approach (ALE) for simulating blast wave propagation in ambient air. Comparisons with experimental results from literature and CONWEP predictions were made in order to validate the numerical model. Several parametric studies were conducted. As a result, the model was explored by the means of an artificial viscosity together with an optimized mesh coarseness, geometry and scaling of explosive mass. Good correlation between the numerical results and experimental data was obtained when using the right combination of solution parameters and multiplying the explosive mass by a factor equal to 1.18. Further simulations must be conducted in order to simulate well the shock wave from an explosive using an ALE formulation (without using a mass-scaling factor). This may be done by modelling the explosive as a spherical shell that contains high-pressured air with specific profiles.

In order to calibrate the numerical models to experimental data, using reasonable fine mesh, explosive mass scaling can be used. Good correlations in terms of pressure and impulse between the numerical results and experimental data were obtained when using the right combination of solution parameters and multiplying the explosive mass by an appropriate scaling factor. As a result, the new simulation procedure model can be utilised to research into the effects of changing the designs of the structure to resist blast pressure loadings.

References

- Aquelet N., Souli M., Olovson L.** (2005): Euler Lagrange coupling with damping effects: Application to slamming problems. *Computer Methods in Applied Mechanics and Engineering*, Vol. 195, pp 110-132
- Benson, D.J.** (1992): Computational Methods in Lagrangian and Eulerian Hydrocodes, *Computer Method Applied Mech. and Eng.* 99, 235-394
- Caramana, E.J., Shashkov, M.J., Whalen, P.P.** (1998): Formulations of artificial viscosity for multidimensional shock wave computations. *J. Comput. Phys.* 144, 70-97.
- Erchiqui F., Souli M., Ben Yedder R.** (2007): Non isothermal finite-element analysis of thermoforming of polyethylene terephthalate sheet: Incomplete effect of the forming stage. *Polymer Engineering and Science*, Volume 47, Issue 12, pp. 2129-2144.
- Gakwaya, A., Sharifi, H., Guillot, M. Souli, M., Erchiqui, F.** (2011): ALE Formulation and Simulation Techniques in Integrated Computer Aided Design: En-

gineering System with Industrial Metal Forming Applications. *CMES: Computer Modeling in Engineering & Sciences* Volume: 73, Issue: 3, Pages: 209-266.

Hallquist, J.O. (1998): LS-DYNA theoretical manual, Livermore Software Technology Company.

Kingery, C., Bulmarsh, G. (1984): Airblast Parameters from TNT spherical air burst and hemispherical surface burst, ARBRL-TR-02555, U.S. Army Ballistic Research Laboratory, Aberdeen Proving Ground, MD.

Longatte L., Bendjeddou Z., M.Souli M. (2003): Application of Arbitrary Lagrange Euler Formulations to Flow-Induced Vibration problems. *Journal of Pressure Vessel and Technology* Vol. 125, pp 411-417.

Longatte L., Verreman V., Souli M. (2009): Time marching for simulation of Fluid-Structure Interaction Problems. *Journal of Fluids and Structures*, Volume 25, Issue 1, , Pages 95-111.

Souli M., Zolesio J.P. (1993): Shape Derivative of Discretized Problems. *Computer Methods in Applied Mechanics and Engineering* 108, pp. 187–199.

Souli M. et al. (2006): High explosive simulation using multi-material formulation. *Applied Thermal Engineering*, 26, 1032-1042.

Young, D.L. (1982): Time-dependent multi-material flow with large fluid distortion, Numerical Methods for Fluids Dynamics, Ed. K. W. Morton and M.J. Baines, Academic Press, New-York.